The Effect of Horizontal Pressure Gradients on the Momentum Transport in Tropical Convective Lines. Part I: The Results of the Convective Parameterization

MARIA FLATAU* AND DUANE E. STEVENS

Department of Atmospheric Sciences, Colorado State University, Fort Collins, CO 80523

(Manuscript received 19 March 1986, in final form 4 February 1987)

ABSTRACT

Measurements of the momentum transport in tropical convective lines suggest that horizontal momentum can be generated by the pressure low located near the center of the convective part of the line.

A simple convective parameterization is used to evaluate this effect. The parameterization is a version of the Fritsch and Chappell scheme, modified in order to evaluate the influence of the horizontal pressure gradients on momentum transport. The results suggest that in modeling of convective (particularly slow-moving) lines with 20 km resolution, subgrid horizontal pressure gradients should be taken into account. Sensitivity studies show that the magnitude of the calculated momentum flux strongly depends on the average vertical velocity and the vertical velocity in clouds.

1. Introduction

A properly formulated parameterization of convection is one of the most important goals in large- and mesoscale modeling. Because the strongest impact of convection on the environment is connected with the release of latent heat, most convective parameterizations emphasize thermodynamic effects of cloud ensembles. However, dynamic effects of convection cannot be neglected. The first step toward formulating a parameterization of those effects is to determine the magnitude and structure of convective momentum fluxes through observations. This can be done by calculating the residual terms in large-scale budget equations, but in the tropics the uncertainty in geopotential field measurements makes this task nearly impossible. However, substantial progress was made after the GARP Atlantic Tropical Experiment (GATE), which provided data with sufficient density and quality for momentum budget calculations.

The first attempt to calculate the momentum budget in the tropical atmosphere was made by Stevens (1979). Using the data from Phase III of GATE (derived from A-scale and A/B-scale ship data), he calculated the vorticity, divergence, and momentum budgets for the average composite synoptic-scale wave. The results of this study showed the existence of large apparent momentum sources in the budget equations, suggesting that subsynoptic-scale circulations strongly affect wave dynamics. The momentum sources in Stevens' study were calculated directly from the momentum equation for the synoptic wave, and geopotential was calculated from the hydrostatic equation and temperature field.

Another approach to the estimation of convective sources of momentum was presented by Sui and Yanai (1986). They calculated vorticity residuals for seven convective events in GATE and then recovered momentum sources using the relation

$$\mathbf{k}\cdot\nabla\times\mathbf{X}=Z \tag{1}$$

where Z is the apparent vorticity source, $\mathbf{X}$ is the momentum source, and $\mathbf{X}$ and Z are calculated as residual terms in large-scale momentum and vorticity equations. If we divide the momentum source $\mathbf{X}$ into the rotational and divergent component ($\mathbf{X}=\mathbf{X}_{\text{rot}}+\mathbf{X}_{\text{div}}$), Eq. (1) allows us to calculate the rotational part of the momentum source. This approach has some deficiencies. First, it is not necessarily true that $\mathbf{X}_{\text{div}}$ is negligible. Second, the interpretation of $\mathbf{X}_{\text{rot}}$ is not clear because $\mathbf{X}_{\text{rot}}$ is not the "apparent" momentum source for any momentum equation. The budget equation for the vorticity source Z contains both the rotational and the divergent component of the wind [cf. Eq. (7) of Sui and Yanai, 1986], and therefore $\mathbf{X}_{\text{rot}}$ is not equivalent to the momentum source for the rotational part of the wind.

As concluded by Stevens (1979), the apparent source of momentum ($\mathbf{X}$) has too complicated a structure to be parameterized by simple formulas like Rayleigh drag [$\mathbf{X}=-D(p)\mathbf{V}$] or diffusion ($\mathbf{X}=K\partial^2\mathbf{V}/\partial z^2$) [where $D(p)$ and K are coefficients]. Since an apparent source of momentum can be attributed to convective activity, a better way to parameterize this effect is to express it in terms of cumulus mass flux and the excess horizontal momentum of cumulus clouds relative to the environ-

* On leave from the Institute of Meteorology and Water Management, Warsaw, Poland.

ment (Yanai, et al., 1973; Schneider and Lindzen, 1976):

$$\mathbf{X} = \frac{\partial}{\partial p} \sum_i \sigma_i \omega_i (\mathbf{V}_{Ci} - \mathbf{V}_E) \tag{2}$$

where the summation is taken over all cloud types (i), σ_i is the fractional area occupied by each cloud type, ω_i is the vertical velocity in pressure coordinates ($m_i = -\sigma_i \omega_i$ is the mass flux in each cloud type), $\mathbf{V}_{Ci}$, $\mathbf{V}_E$ represent horizontal velocity in the cloud and in the environment, respectively. Equation (2) expresses the apparent momentum source in terms of the vertical flux of the horizontal momentum. The contribution of the horizontal fluxes of horizontal momentum to the convective momentum source can be neglected (Cotton and Anthes, 1986). As shown by Shapiro and Stevens (1980) the Eq. (2) can be written in the bulk form:

$$\mathbf{X} = \delta(\mathbf{V}_C - \mathbf{V}_E) + \left[M_C \frac{\partial \mathbf{V}_E}{\partial p} + \sigma(\nabla \phi)_C \right]. \tag{3}$$

In this formulation, the first term describes the detrainment of momentum to the environment (δ is the detrainment coefficient), $M_C(\partial \mathbf{V}_E)/\partial p$ describes the effects associated with compensating environmental subsidence caused by the convective activity, and $\sigma(\nabla \phi)_C$ describes the cloud-scale horizontal pressure gradients. A one-dimensional cloud model is used to calculate $\mathbf{V}_C$, M_C and δ. The term involving cloud-scale pressure gradients is usually neglected.

Equation (3), with the assumption that $\sigma(\nabla \phi) = 0$ was used by Shapiro and Stevens (1980) to calculate convective momentum fluxes in order to compare them with the apparent momentum sources from Stevens' (1979) large-scale momentum budget calculations. The results showed some inconsistencies between parameterized and observed convective momentum sources, although the same comparison for vorticity showed much better agreement. Shapiro and Stevens suggested that the momentum fluxes depend much more on the organization of the convective system than vorticity fluxes do. The assumption that the influence of the cloud-generated pressure forces on momentum flux is negligible can be justified in the case of strictly random convection, but it is questionable for highly organized convective systems such as convective lines.

Indeed, aircraft measurements of momentum flux in GATE convective lines documented by LeMone (1983) and LeMone et al. (1984) suggested that although the momentum fluxes for isolated clouds or less-organized convective lines do not show the influence of pressure gradients, the momentum flux in two-dimensional convective lines is strongly affected by the horizontal pressure gradient force. In GATE, the fluxes of horizontal momentum perpendicular to the line were always negative (where horizontal wind is defined to be positive in the direction of the line motion), showing in many cases an upgradient (i.e., acting to increase the shear) transport of momentum. LeMone et al. (1984) argued that taking into account this kind of momentum transport in the convective lines observed in GATE would improve Shapiro and Stevens' (1980) results and bring parameterized values of apparent momentum sources closer to those calculated from large-scale budgets.

LeMone's observational results were supported by the results of the numerical study of the momentum generation in the tropical convective line presented by Soong and Tao (1984). They used a two-dimensional cloud ensemble model to simulate the formation of an ensemble of clouds under the given large-scale conditions. The momentum flux perpendicular to the line ($\overline{u'w'}$) appeared to be extremely sensitive to the details of simulations, as was the cloud configuration produced by the model. Since the momentum flux in the direction parallel to the line ($\overline{v'w'}$) was insensitive to simulation details, they concluded that the pressure force associated with the cloud configuration caused such dramatic changes in the u-momentum flux.

The results presented by LeMone (1983) and LeMone et al. (1984) also showed that most of the momentum generation by horizontal pressure gradients occurs in the convective part of the line: the narrow (20–40 km) zone behind the leading edge. This suggests that convection-generated pressure forces can cause problems not only in large-scale models, but also in mesoscale models. However, the convective parameterizations used in mesoscale models also make the assumption that horizontal momentum in clouds is conserved (Raymond, 1984; Beniston, 1984; Fritsch and Chappell, 1980a,b). It is the goal of this study to analyze the error associated with neglecting the cloud-scale pressure forces in parameterization of convective momentum flux. In Part I we approach this problem using Fritsch and Chappell's (1980, hereafter FC) parameterization and the data for the GATE two-dimensional convective lines. Part II further treats the parameterization problem by considering the influence of the pressure gradient on the behavior of individual Lagrangian parcels.

2. Data and computational design

a. Fritsch and Chappell parameterization

The FC parameterization is based on a local consumption of the available buoyant energy. It was designed for use in mesoscale models with resolution about 20 km. The mesoscale model provides temperature, humidity, and vertical velocities at a given grid point. If the mesoscale model generates positive available buoyant energy (CAPE) at this grid point, convection is assumed to entirely remove this energy in the specified period of time τ_c. Time scale τ_c is estimated as the time needed for clouds to move through the grid element, by dividing grid length by the mean environmental wind speed.

To determine the amount of convection (updraft and downdraft area), the following iterative procedure is used. Initially it is assumed that updraft occupies 1% of the grid area. Cloud properties are calculated. The fraction of downdraft air corresponding to the initial unit of updraft air is estimated from water-budget considerations. Environmental compensating subsidence is calculated from the mass continuity equation:

$$A_E w_E \rho_E = A\bar{w}\bar{\rho} - A_U w_U \rho_U - A_D w_D \rho_D \qquad (4)$$

where A is the area of the grid box, and the subscripts E, U, D identify environment, updraft and downdraft respectively. The new values of variables in the grid area A are evaluated as the average over updraft, downdraft and environment area. If the new buoyant energy is larger than zero, a larger area of updraft is assumed and the calculation is repeated. This iterative procedure is continued until all buoyant energy is used for convection.

The cloud model used in FC parameterization is one-dimensional and consists of a steady-state plume convective updraft and steady-state plume convective downdraft. It is assumed that the mass transport in the updraft increases linearly with height from the cloud base to the cloud top. Similarly, the downdraft mass transport increases linearly from the level of free sink to the surface. Midcloud detrainment is neglected for both updraft and downdraft.

b. *Data and modification of the Fritsch and Chappell parameterization*

Most of the changes we made in the original FC formulation were necessitated by our use of GATE observations, rather than a numerical model, to supply the input values for the parameterization, and our desire to take into account the observed pressure gradient forces. Some additional changes were required because we consider tropical and not midlatitude convective systems, as in FC.

We consider the quasi-two-dimensional GATE composite for slow and fast convective lines, and perform our calculations for the convective part of the line. We assume that the convective part of the line is contained in a mesoscale "grid box" of size d. The buoyant energy in this box is calculated using the composite soundings for the slow- and fast-line environments shown in Fig. 1. The data are displayed using a right-handed coordinate system, moving with the line. Axis x is normal to the line with the positive sign in the direction of the line movement, and axis y is parallel to the line. Observed pressure disturbance fields for the fast and slow lines (Fig. 2) provide subgrid pressure gradients.[1] Horizontal pressure gradients along the line axis are assumed equal to zero. Due to the lack of data above 6 km, we assume that the perturbation pressure forces above this level are negligible.

According to Barnes and Sieckman (1985), the convectively active region of the line occupies roughly a 20–40 km wide zone normal to the leading edge. Barnes and Sieckman's (1985) calculations show that in this region the buoyant energy is significantly reduced (96% in the fast and 66% in the slow composite line). It is worth noting that Barnes and Sieckman's calculations are performed in the coordinate system moving with the line. Therefore, the reduction of buoyant energy along the x-axis is equivalent to the temporal change of buoyant energy above a fixed geographical location. The time scale for such a change is therefore $\tau_c = d/c$, where d is the width of the convective region and c the speed of the line. Our hypothetical model "grid box" contains the convective part of the line. For simplicity we assume the same size of the box for the fast and slow convective lines, i.e. $d = 30$ km. The speed of the lines is known from observation and is equal to 3 m s^{-1} for the slow and 12 m s^{-1} for the fast composite convective line. We assume that during the time $\tau_c = d/c$, the buoyant energy is reduced by 80% (instead of 100% as assumed by FC).

The reduction of buoyant energy is achieved primarily by changes in the environment caused by the compensating subsidence w_E. In order to evaluate w_E, it is necessary to know the mean vertical velocity in the considered grid area [according to Eq. (4)]. Since from the GATE data we cannot obtain the full profile of the mean mesoscale $\bar{w}$ in the convective part of the line, and assuming $\bar{w} = 0$ in this region would not be reasonable, we use the following procedure to determine compensating subsidence w_E. As illustrated in Fig. 3, we assume that the compensating subsidence corresponding to the updrafts and downdrafts in our "grid box" (with the area $A = A_U + A_D + A_E$) can occur in an area larger than the "grid box"; i.e., in the area $A + A_2$. Therefore, w_E is calculated according to the formula

$$\begin{aligned}(A_E + A_2) w_E \rho_E &= (A + A_2)\bar{w}\bar{\rho} - A_U w_U \rho_U - A_D w_D \rho_D \\ &= 0 - A_U w_U \rho_U - A_D w_D \rho_D. \qquad (5)\end{aligned}$$

We also test the parameterization using Eq. (4) with different mesoscale velocities in order to evaluate the sensitivity of calculated momentum fluxes to the method of evaluating the compensating subsidence [Eq. (4) or Eq. (5)] and the magnitude of the mesoscale vertical velocity.

The cloud model used in the parameterization is equivalent to that described by FC except with these modifications:

1) Rather than calculate the water budget with rain efficiency determined from the wind shear, as perhaps appropriate for middle latitudes, we use the water budget obtained by Gamache and Houze (1983) in their

[1] The fields in Fig. 2 are called the "mesoscale pressure fields" by LeMone et al. (1984). We avoid this term because of possible confusion with the "mesoscale grid box".

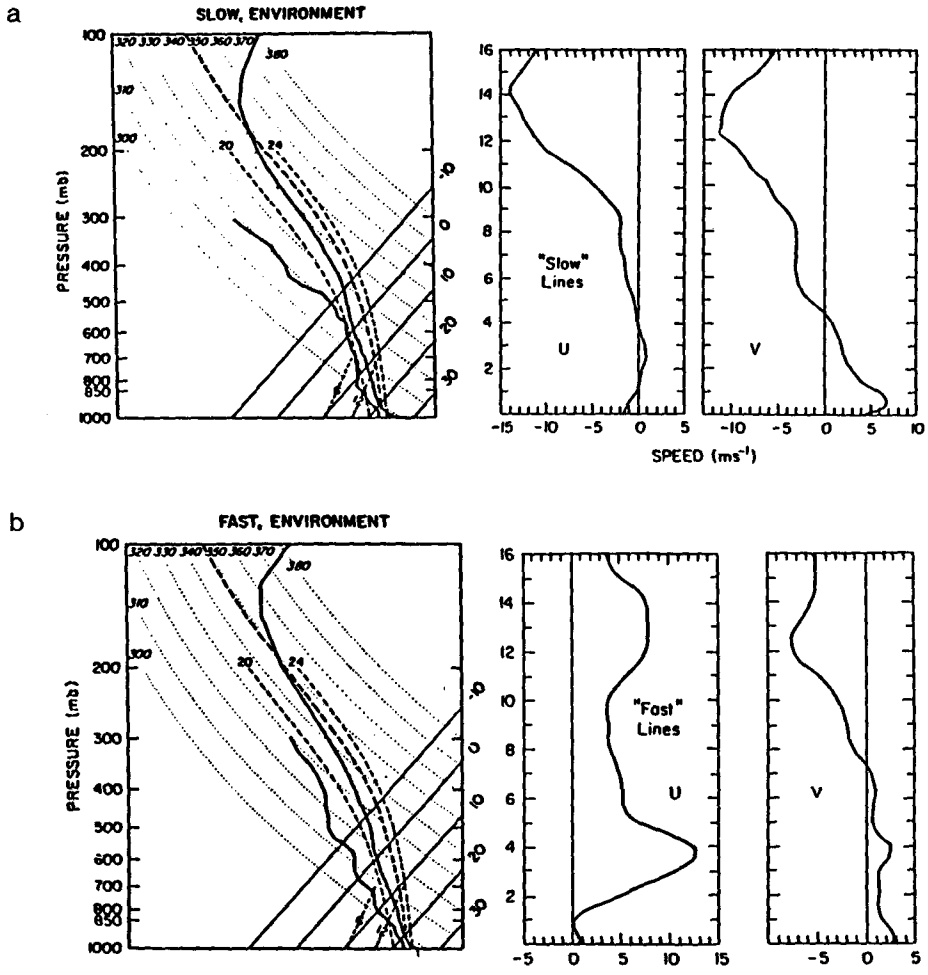

FIG. 1. Composite environmental sounding and horizontal wind used in the parameterization for the (a) slow line and (b) fast line (from Barnes and Sieckman, 1985).

observational study of convective systems in GATE (Fig. 4).

2) Following Anthes (1974) and Frank and Cohen (1985), liquid water drag, mixing of vertical momentum and the virtual mass effect are taken into account in the vertical momentum equation.

3) The cloud horizontal momentum equation includes the pressure gradient force. Thus the cloud budget of horizontal momentum has the form (Shapiro and Stevens, 1980)

$$\frac{\partial(M_C u_C)}{\partial z} + \delta u_C - \epsilon u_E = \sigma \nabla p \qquad (6)$$

where ϵ and δ are entrainment and detrainment coefficients (following FC we assume $\delta = 0$); σ is the fractional area occupied by convection and is calculated as a ratio of mass flux to the vertical velocity in the convective draft; $\sigma \nabla p$ is the horizontal pressure gradient force.

According to LeMone (1983), the updraft cores tend to occur between the leading edge and the pressure low, and downdraft cores are observed behind the low (Fig. 5). Therefore, in this study, pressure gradient forces acting on updraft (downdraft) are assumed to have opposite signs and are calculated at every level as $\Delta p/\Delta x$, where Δp is the pressure difference between the lowest pressure and pressure at the front (rear) of the "grid box" and Δx is the corresponding distance. For purposes of this study, we take the pressure field from observations. In a complete parameterization (i.e., a parameterization used in a numerical model) the cloud-scale pressure field must be calculated within the parameterization scheme.

3. Results

Vertical fluxes of horizontal momentum depend on cloud mass flux, wind shear, pressure forces, and vertical velocity in the updraft (downdraft) which deter-

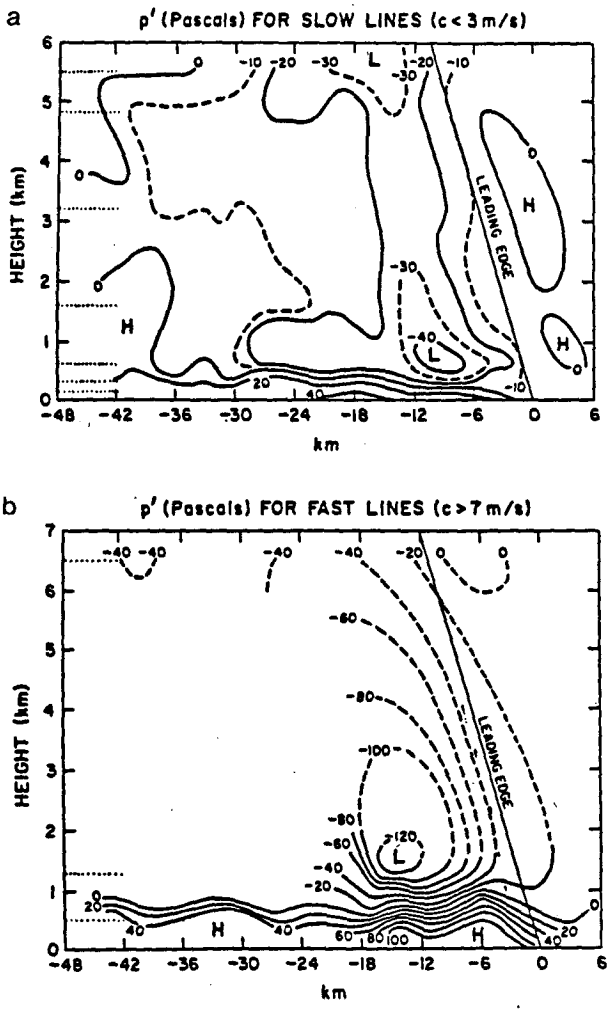

FIG. 2. Composite pressure disturbance field for the (a) slow and (b) fast GATE convective lines (from LeMone et al. 1984).

mine the time over which the pressure gradient force acts on updraft (downdraft) parcels. In section 3a we present the influence of the horizontal pressure gradients on the momentum flux in the slow and fast convective lines. For both types of lines, we use the condition that the mesoscale vertical velocity is constant with height and equal to zero in the extended area ($A + A_2$). Compensating subsidence is allowed to occur on an area four times larger than the area of the convective region ($A_2 = 4A$). In section 3b we compare our results with GATE observations. In particular, we discuss factors influencing cloud mass flux (e.g., assumptions concerning mesoscale vertical velocity) which in turn determines the magnitude of the momentum flux. In section 4 we consider the implications of our findings for mesoscale numerical models.

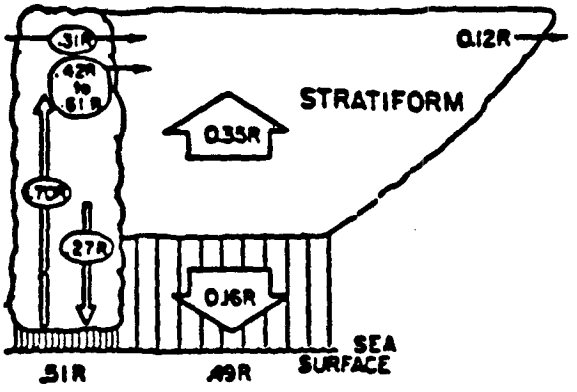

FIG. 4. Schematic diagram of the squall-system water budget (from Gamache and Houze, 1983).

a. *The influence of the horizontal pressure gradients on the momentum flux*

As we mentioned before, the influence of the horizontal pressure force on the momentum of the updraft (downdraft) parcels depends on the vertical velocity in the updraft (downdraft). The vertical velocities calculated in FC parameterization from the vertical mo-

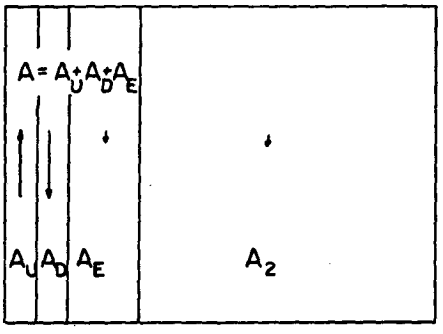

FIG. 3. Schematic diagram of area of the calculations.

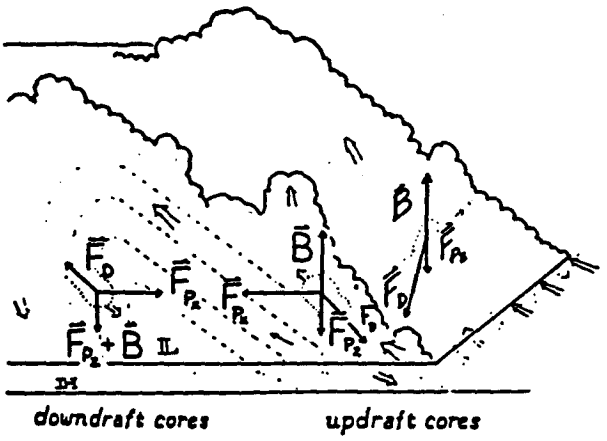

FIG. 5. Schematic of the processes leading to momentum generation in the convective band (from LeMone, 1983).

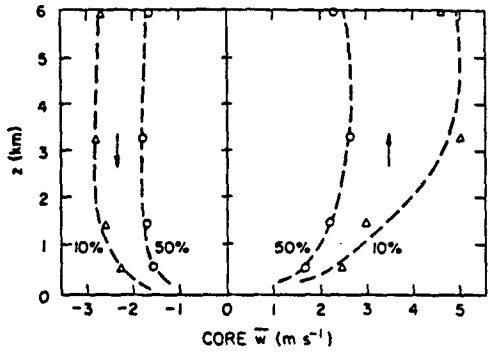

FIG. 6. Vertical velocity in the GATE convective cores (from LeMone and Zipser, 1980).

mentum equation reach 15 m s^{-1}, which is much too large compared to vertical velocities measured in the GATE convective cores which have the median value about 2 m s^{-1} (Fig. 6). A similar problem was reported by Zipser and LeMone (1980). Despite the use of different cloud models, different soundings, and different initial conditions, they were not able to obtain realistic vertical velocities and realistic cloud top heights simultaneously. Zipser and LeMone attribute this difference to the fact that the true "environment" of the convective cores is defined not by the sounding some tens of kilometers ahead of the convective line, but by the "mesoscale" conditions within the convective line itself.

Because of this large difference between calculated and measured vertical velocity in clouds, we calculate the momentum flux using three alternative assumptions which are summarized in Table 1. In experiment A we neglect the horizontal pressure gradients. In experiments B and C the horizontal pressure gradients are taken into account but we use different values of the vertical velocity in convective drafts. Vertical velocities in experiment B are calculated in the parameterization from the vertical momentum equation, while in experiment C the cloud vertical velocities are modified to match approximately the observations in the GATE convective cores. The cloud mass flux within a grid box is the same in all three experiments, because it depends only on the mass flux at cloud base and the amount of mass entrained from the environment. The fractional area occupied by updraft depends on mass flux and vertical velocity within the cloud updraft according to the formula

$$\sigma_U \equiv A_U/A = M_U/(\rho_U w_U). \tag{7}$$

A corresponding relationship holds for downdrafts.

The results for the slow and fast convective line experiments are shown in Figs. 7 to 11. Equation (7) and the comparison of the calculated and measured vertical velocities in convective drafts (Fig. 7) suggest that the area occupied by convection is much larger when the vertical velocities from GATE measurements (Experiment C) are used. Figure 8 demonstrates this model hypothesis conclusively. It also can be seen from Fig. 8 that the fractional area for the fast line is 2.5 times that for the slow line. Since vertical velocities in updrafts are similar for slow and fast lines, Eq. (7) implies a corresponding ratio of 2.5 for the mass fluxes. This result is similar to Barnes and Sieckman's (1985) observations (3:1 upward mass flux ratio for fast and slow convective lines).

The momentum fluxes produced separately by the updraft and the downdraft are shown in Figs. 9 and 10, respectively. Comparison of Figs. 9 and 10 indicates that the momentum flux generated by the downdraft is about an order of magnitude smaller than the momentum flux generated by the updraft. This results from the fact that the calculated convective-scale downdraft mass flux itself is an order of magnitude smaller than the updraft mass flux.

From Equations (2) and (3) it is clear that the cloud-induced horizontal force **X** depends strongly on the environmental wind shear ($\partial \mathbf{V}_e/\partial p$). Because the slow-moving lines are roughly aligned so as to maximize the vertical shear parallel to their axes (LeMone et al., 1984, Fig. 1), the momentum flux perpendicular to the line $\overline{u'w'}$ (Fig. 9), without horizontal pressure forces is much smaller than the along-line momentum flux $\overline{v'w'}$ (Fig. 11). Furthermore, $\overline{u'w'}$ changes sign according to the changes in the environmental wind. When the pressure gradient forces are taken into account, the momentum flux $\overline{u'w'}$ becomes larger and negative. This effect is about two times stronger when we consider vertical velocities representative of GATE convective cores.

The momentum flux for the fast line is about ten times larger than for the slow line (Fig. 9). This can be explained by the presence of the larger mass flux and stronger shear in the u velocity. Horizontal pressure gradients in the fast convective line are stronger than those in the slow line, and also act to increase the magnitude of the momentum flux, but they do not significantly change the shape of the momentum flux profile, as in the case of the slow line. Because in the fast line, low-level shear in the horizontal wind parallel to the line is small, $\overline{v'w'}$ momentum fluxes below 6 km are

TABLE 1. Summary of the numerical experiments.

Experiment	Pressure gradient force	Vertical velocity in convective drafts
A	0	—
B	$-\frac{\Delta p}{\Delta x}$	calculated in FC parameterization
C	$-\frac{\Delta p}{\Delta x}$	observed in GATE

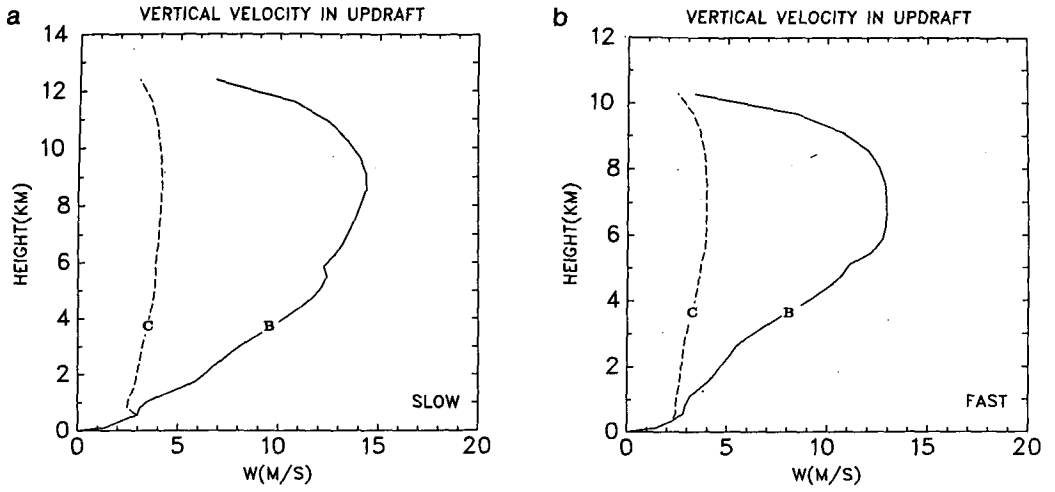

FIG. 7. Vertical velocity in updraft for the (a) slow convective line and (b) fast convective line; solid line: calculated from the vertical momentum equation in the FC parameterization; dashed line: modified to match GATE data.

smaller than $\overline{u'w'}$ and have magnitudes similar to those in the slow line (Fig. 11).

The results of experiments B and C show that the change of momentum flux, caused directly by horizontal pressure gradient, depends strongly on vertical velocity in clouds. Therefore, to account properly for the effect of the horizontal pressure gradient, it is necessary to use a parameterization which produces realistic vertical velocities.

The horizontal forces resulting from cloud momentum transports are given by vertical divergence of the momentum fluxes, which are shown in Fig. 12. The derivative of the momentum flux in the fast line (Fig. 12b) is about ten times larger than in the slow line (Fig. 12a). A comparison of the vertical derivative of the momentum flux calculated with (B, C) and without (A) pressure gradients for both types of lines indicates that the momentum flux derivative shows relatively less dependence on the horizontal pressure gradient for the fast line. The maximum error caused by neglecting the horizontal pressure gradient (i.e., C–A) is, in the case of slow line, of the same magnitude as the force calculated without pressure gradients (Fig. 12a, experiment A). In the case of the fast line, the error is about three times smaller than the momentum flux divergence.

The comparison in Fig. 13 of the component of the vertical divergence of the momentum flux connected with the shear in the environmental wind $\partial(M_C u_E)/\partial z$, with the component describing the vertical change in

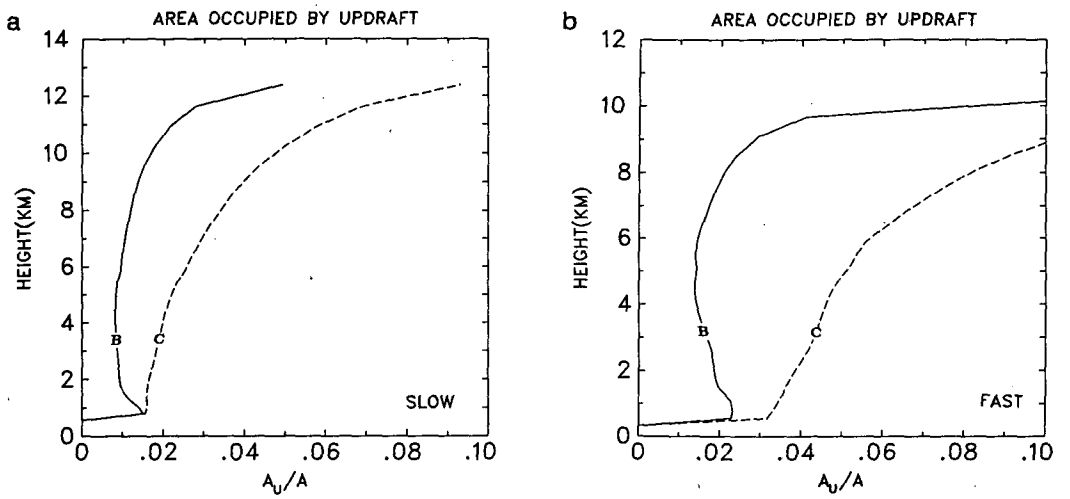

FIG. 8. Fraction of the grid area occupied by the updraft: for the (a) slow line and (b) fast line. Solid line: calculated with vertical velocity obtained in parameterization; dashed line: calculated with observed vertical velocity.

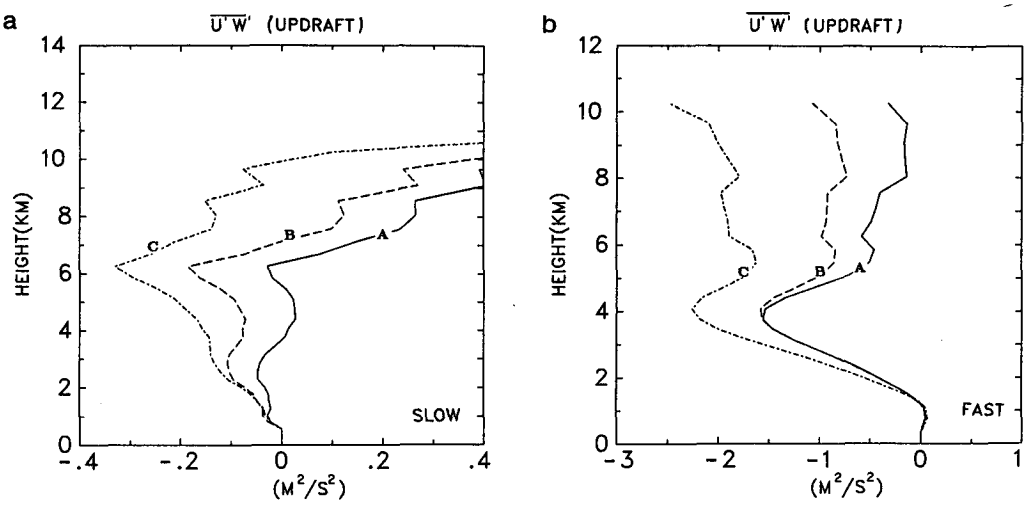

FIG. 9. Horizontal momentum flux $\overline{u'w'}$ due to the updraft in the (a) slow line and (b) fast line. Solid line: Experiment A; dashed line: Experiment B; dot-dashed line: Experiment C.

the horizontal velocity in clouds $\partial(M_C u_C)/\partial z$, explains why the slow line is influenced more strongly by the pressure gradients. In the slow convective line, vertical shear in the u-velocity is small; when the horizontal pressure forces are taken into account, $\partial(M_C u_C)/\partial z$ is comparable in size with $\partial(M_C u_E)/\partial z$. In the fast convective line, the changes in the cloud velocity caused by horizontal pressure gradients are larger than in the slow line, but the shear in the direction parallel to the line is strong; hence, the $\partial(M_C u_E)/\partial z$ term dominates. It is worth noting, however, that although $\partial(M_C u_E)/\partial z$ is connected with the environmental wind shear, it does not act to eliminate the maximum in the horizontal wind (as simple diffusion or Rayleigh friction would). Because the force term due to cumulus friction is related to the first derivative of u_E, rather than the second or zeroth derivative, it acts primarily to lower the jet.

b. Comparison with the GATE measurements

Some examples of the momentum fluxes measured in GATE fast and slow convective lines (LeMone et al., 1984) are shown in Fig. 14. Observed fluxes are normalized to 100 km-long flight legs. Since most of the momentum flux is created in the convective part of the line, we expect momentum flux in the first 30 km behind the leading edge to be significantly larger than that averaged over 100 km. Comparison of Figs. 9 and 11 with the momentum fluxes in Fig. 14 shows that below 6 km momentum fluxes calculated in the

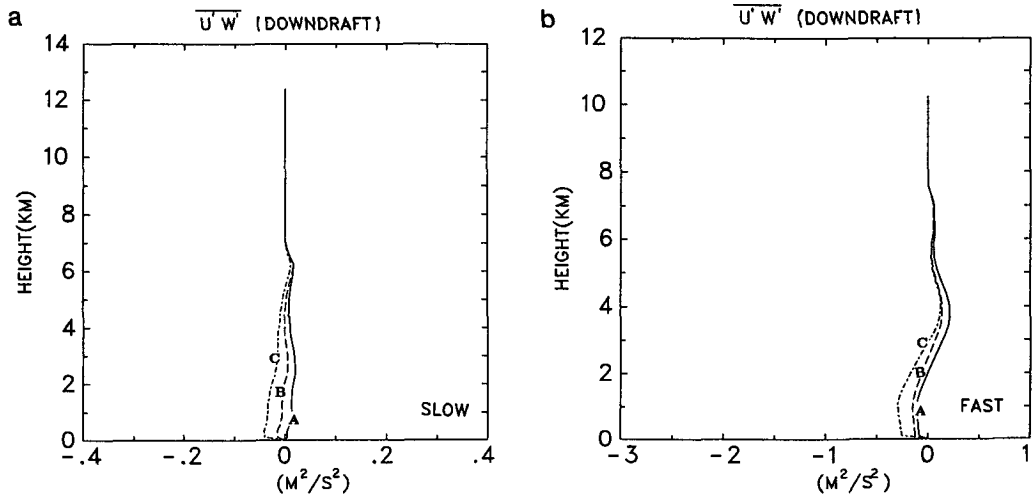

FIG. 10. Horizontal momentum flux $\overline{u'w'}$ due to the downdraft for the (a) slow line and (b) fast line. Solid line: Experiment A; dashed line: Experiment B; dot-dashed line: Experiment C.

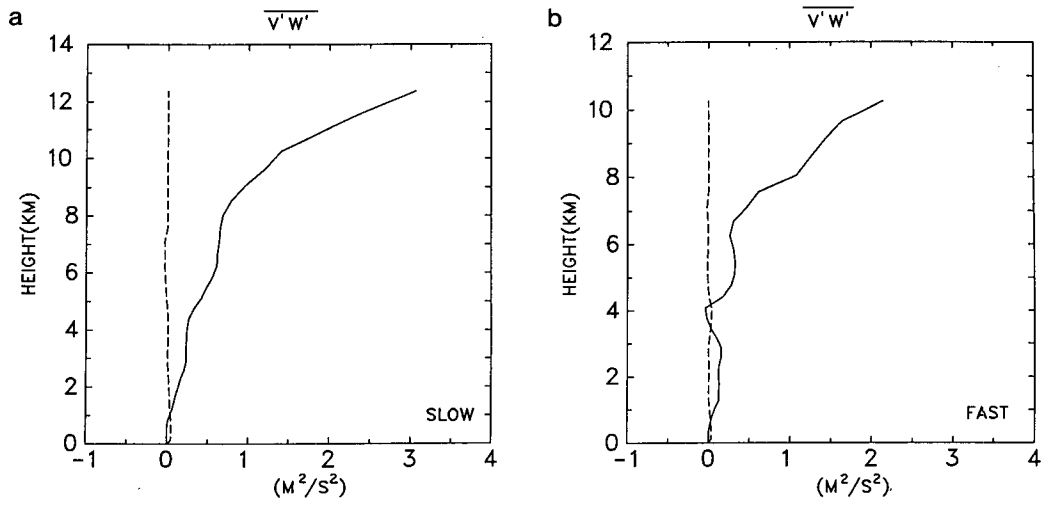

FIG. 11. Horizontal momentum flux $\overline{v'w'}$: solid line: generated by updraft, dashed line: generated by downdraft; (a) in the slow-moving line and (b) in the fast-moving line.

parameterization[2] are even smaller than the 100 km averages from GATE. It is worth noting however, that this underestimation of the momentum flux is similar for both line types and for both $\overline{u'w'}$ and $\overline{v'w'}$ momentum fluxes. According to the GATE measurements, the momentum flux in fast lines is about ten times larger than in slow lines. That fact agrees with our results in Fig. 9. Also, $\overline{v'w'}$ momentum fluxes are underestimated in the same degree as $\overline{u'w'}$. This suggests that it is the mass flux which is responsible for the underestimation of the momentum flux, since mass flux is the common element of the calculation for each direction.

Indeed, even when we use the observed vertical velocity in convective cores, the area occupied by the active convection calculated from the FC parameterization is still much smaller than the area occupied by convective cores measured in GATE. Table 2 shows the fractional length of the GATE aircraft legs occupied by convective cores (Zipser and LeMone, 1980). Since roughly all convective cores occur in the convective part of the line, the fractional coverage by convective cores of the first 30 km behind the leading edge should appear as in Table 3. The results shown in Table 2 are based on the measurements of different types of lines. To determine how our parameterization underestimates mass flux, we average the fractional coverage by updrafts for both types of lines from Fig. 8 and list the parameterized averages along with "observed" averages in Table 3. It appears that the results of the parameterization are about four times smaller than the values measured in GATE. Since we use the vertical velocity in convective cores based on the GATE measurements, it suggests that our mass flux is also about four times too small. We offer the following hypothesis for this discrepancy.

The updraft mass flux at the cloud base in the FC parameterization is iterated until the available buoyant energy (CAPE) in the grid area is equal to zero. The reduction of CAPE is achieved by the combination of the cooling of the layers close to the surface and the warming of the higher layers. The change in the grid area temperature depends mainly on compensating subsidence. Only close to the ground does the spreading convective downdraft cause significant cooling of the lowest layer (Fig. 15). Therefore, the cloud mass flux calculated in the FC parameterization depends primarily on parameters influencing the compensating subsidence. From mass continuity [Eq. (4)] we note that if the mesoscale vertical velocity $\bar{w}$ is positive, the same updraft mass flux causes smaller compensating subsidence than that which occurs in the case with zero mean vertical velocity. This means that an increase in the mean vertical velocity will increase the cloud mass flux needed to reduce APE. In addition, when the mean vertical velocity increases with height, heating of the higher layers is smaller and the updraft mass flux needed to reduce the APE has to be even larger than in the former case.

To determine how the mass flux calculated in the FC parameterization depends on $\bar{w}$, we run the parameterization using mass continuity [Eq. (4)] and different (arbitrarily chosen) mesoscale vertical velocities shown in Fig. 16a. It can be seen from Figs. 16b and 16c that the mean mesoscale vertical velocity is a very important factor in the calculation of the convective heating and the cloud mass flux. Figure 17 shows that the vertical velocity in the slow convective line averaged over the first 30 km behind the leading edge can be even larger than that used in the sensitivity test pre-

[2] Large values of the calculated momentum flux above 6 km are the result of assuming $\delta = 0$.

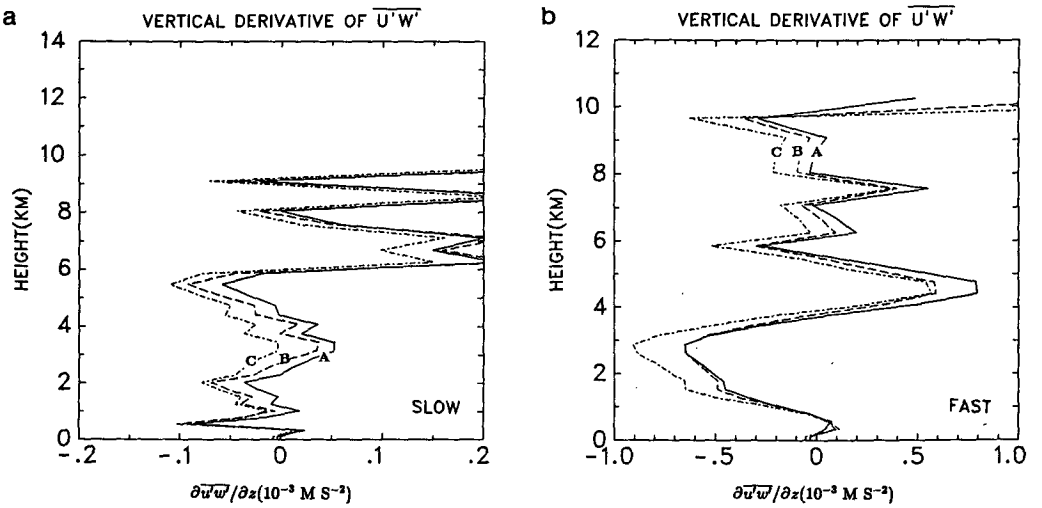

FIG. 12. Vertical derivative of the horizontal momentum flux and for the (a) slow-moving line and (b) fast-moving line. Solid line: Experiment A; dashed line: Experiment B; dot-dashed line: Experiment C.

sented above. On the other hand, the mass flux calculated with the continuity equation (5) is larger than that for $\bar{w} = 0$, but smaller than that for $\bar{w} = 8$ cm s^{-1}. Therefore, our assumption of additional compensating subsidence did not sufficiently improve our results. Because of the lack of data above the 6 km level, we did not try to reproduce the convective heating and mass flux using the mesoscale vertical velocity from Fig. 17. We believe that a nonrealistic $\bar{w}$ is the source of our underestimation of the cloud mass flux and momentum flux.

Figure 18 shows the comparison of the momentum flux for the slow line calculated with the correction for a realistic (i.e., increased four times as suggested by comparison with observations) mass flux, with the momentum flux measured in the slow line observed during GATE on 14 September 1974 (LeMone, 1983). The data for the 14 September line are averaged over the first 30 km behind the leading edge. It can be seen that *the pressure forces play a dominant role in creating the momentum flux which resembles that measured in* GATE. Calculated momentum flux, even after correc-

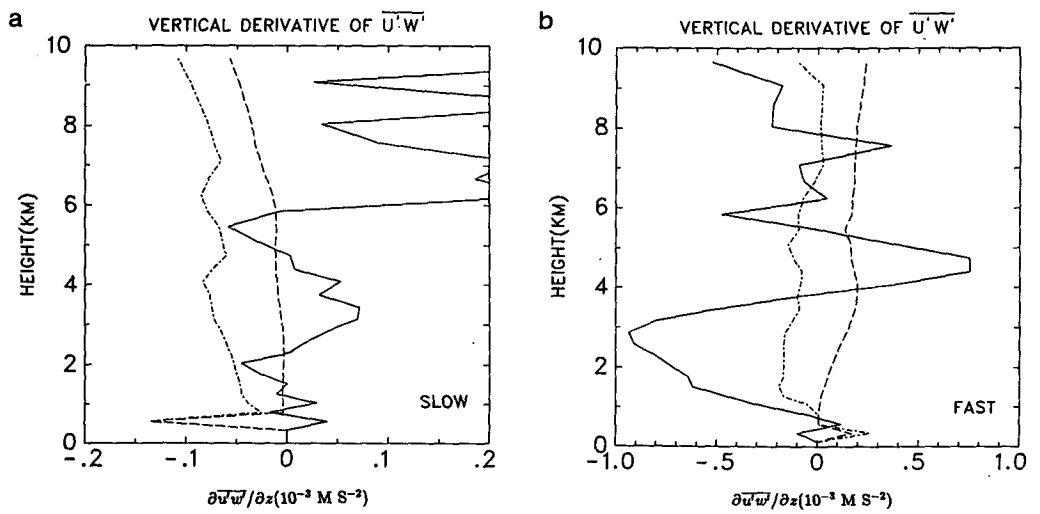

FIG. 13. Components of the momentum flux derivative $\partial[M_c(u_c - u_E)]/\partial z$ for the (a) slow and (b) fast convective line. Solid line indicates $\partial(M_c u_E)/\partial z$, dashed line indicates $\partial(M_c u_c)/\partial z$ for the case without horizontal pressure gradients, dot-dashed line indicates $\partial(M_c u_c)/\partial z$ with horizontal pressure gradient.

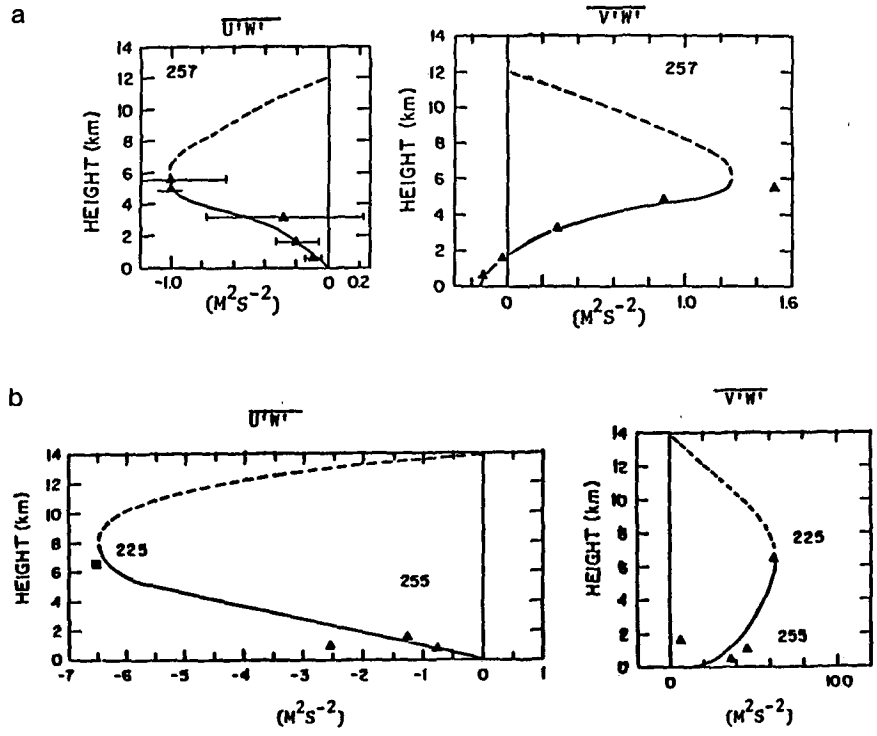

FIG. 14. Momentum fluxes for the (a) slow and (b) fast convective lines as measured in GATE (from LeMone et al., 1984). The data are averaged over 100 km-long flight legs.

tions for pressure forces and realistic mass flux, is still smaller than the momentum flux of the 14 September line, possibly as a result of our comparing momentum flux calculated for the *composite* slow line with the momentum flux for a *particular* case.

4. Discussion and conclusions

The problem with mean mesoscale vertical velocity is avoided in numerical models, where $\bar{w}$ is supplied by the model itself. The other factors (e.g., lateral detrainment, low-level cooling) do not drastically change the mass flux calculated in the parameterization. Hence, we believe that the parameterization used in a numerical model which presumably predicts realistic $\bar{w}$ should produce reasonable magnitudes of mass and momentum fluxes. It is worthwhile to determine the influence of the subgrid pressure gradients on the mean mesoscale wind in comparison with other terms in the mesoscale momentum equation (averaged over 30 km):

$$\frac{\partial \bar{u}}{\partial t} = -\frac{1}{\bar{\rho}}\frac{\partial \bar{p}}{\partial x} - \bar{u}\frac{\partial \bar{u}}{\partial x} - \bar{w}\frac{\partial \bar{u}}{\partial z} + F_c + F_{cp}. \quad (8)$$

Here the overbar denotes the average over 30 km, F_c is the convective-scale momentum flux calculated without the subgrid pressure gradient force, and F_c

TABLE 2. Fractional length of aircraft legs occupied by drafts and cores (from Zipser and LeMone, 1980).

Altitude range (m)	Drafts		Cores	
	Up	Down	Up	Down
4300–8100	0.169	0.299	0.46	0.18
2500–4300	0.183	0.303	0.48	0.37
700–2500	0.163	0.252	0.21	0.11
300–700	0.166	0.188	0.15	0.08
0–300	0.159	0.157	0.03	0.02

TABLE 3. Comparison of the observed and calculated fractional length of the convective region occupied by updraft cores. Observed values are obtained by multiplying the values from Table 2 by the ratio of the length of aircraft leg (100 km) to the assumed length of convective region (30 km). The parameterized values are averaged for slow and fast line (Fig. 8).

Altitude range (m)	Updraft cores (observed)	Updraft cores (parameterized)
4300–8100	0.153	0.043
2500–4300	0.153	0.031
700–2500	0.070	0.023
300–700	0.050	—
0–300	0.010	—

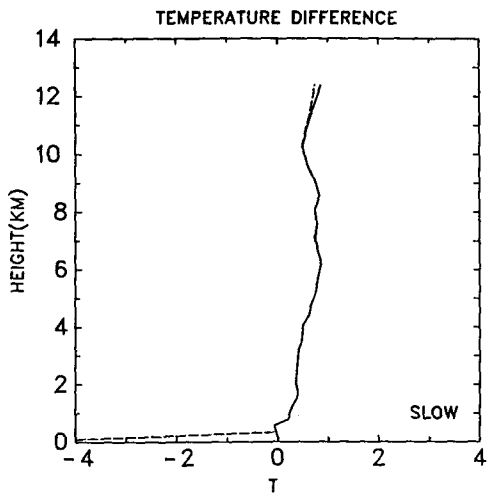

FIG. 15. Difference between the initial temperature of the environment and the following: the temperature after parameterization averaged over the grid area (dashed line), the environmental temperature after the parameterization (solid line).

$+ F_{cp}$ is the momentum flux calculated with the pressure gradient force. The average pressure gradient and average advective terms are estimated from the observational data for the 14 September 1974 slow convective line (LeMone, 1983). The convective momentum flux is calculated using FC parameterization and corrected for the observed mass flux. Figure 19 shows the profiles of different terms in Eq. (8). It can be seen that the effect of the horizontal pressure gradient (solid line in Fig. 19) has a magnitude comparable with the other terms in the momentum equation. It seems that in the slow-moving convective line, the horizontal pressure gradient in the cloud momentum flux parameterization has a significant impact on the mesoscale dynamics.

The main purpose of this study was to evaluate the influence of the subgrid horizontal pressure gradients on convective momentum fluxes in two-dimensional tropical convective lines. We have shown that in 2-D convective lines, especially the slow moving lines, the horizontal pressure forces play a crucial role in creating a momentum flux similar to that observed in GATE. For the slow-moving line, it is impossible to obtain either the observed magnitude or the sign of momentum flux, unless the subgrid horizontal pressure gradient effect is included. The influence of the pressure forces on momentum flux strongly depends on vertical velocities in the convective draft.

We have also compared the various terms in the u momentum equation averaged over 30 km, concluding that the change of the vertical divergence of the subgrid momentum flux caused by subgrid scale horizontal pressure gradient has magnitude comparable with the other terms in the momentum equation. This result

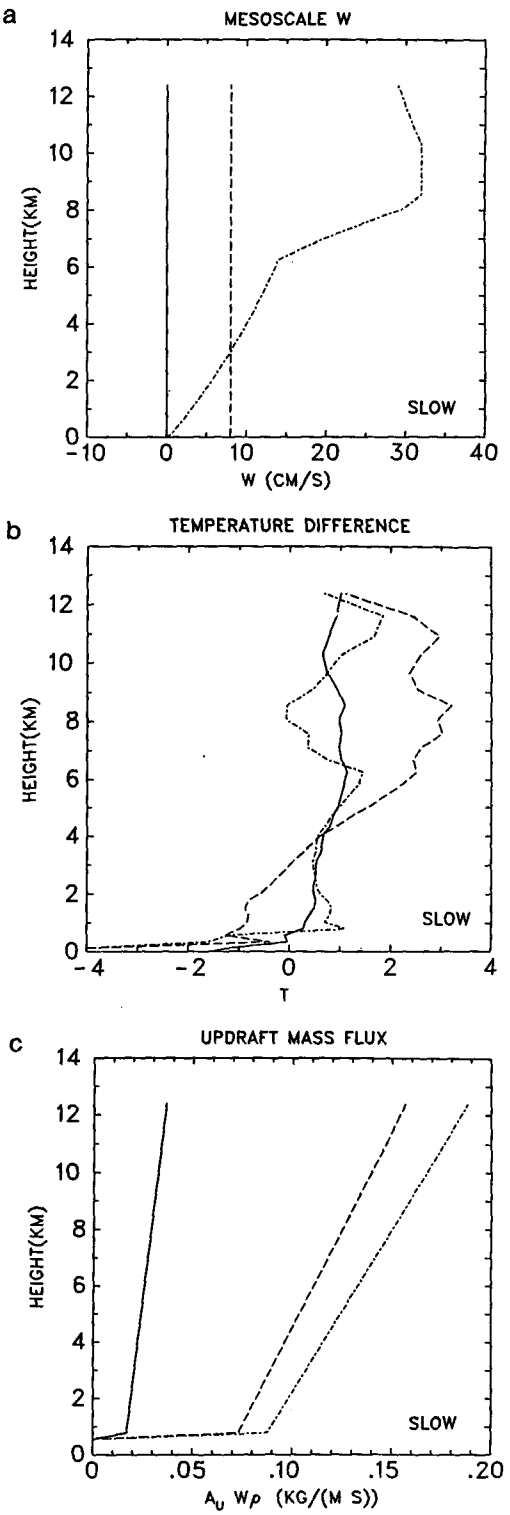

FIG. 16. Sensitivity of the calculated mass flux to the change in the mesoscale mean velocity. (a) mesoscale $\bar{w}$ assumed in the sensitivity test, (b) change in the grid-box temperature obtained for different $\bar{w}$ from (a), (c) momentum fluxes calculated with the different $\bar{w}$'s from (a). The different line patterns in (b) and (c) indicate values calculated with the $\bar{w}$ indicated by the same line pattern in (a).

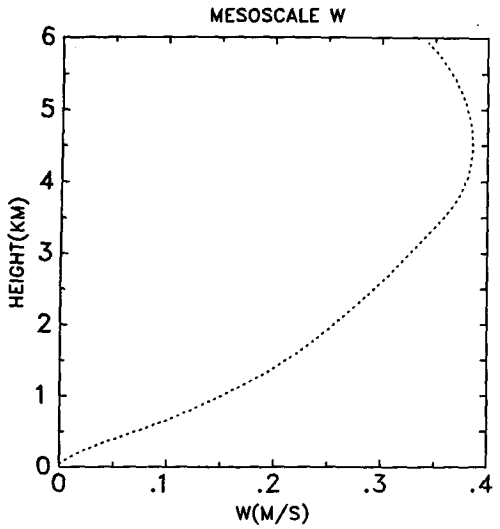

FIG. 17. Vertical velocity in the 14 September convective line (LeMone, 1983) averaged over first 30 km behind the leading edge.

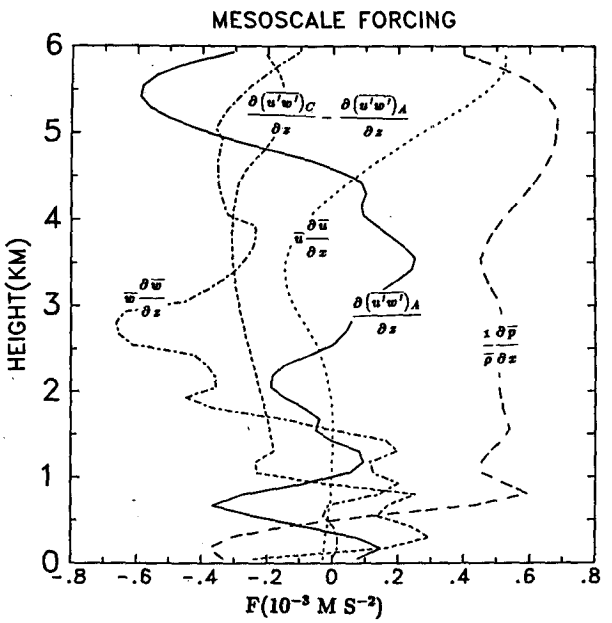

FIG. 19. Comparison of the change in the vertical derivative of the momentum flux generated by convection with other terms in the mesoscale u-momentum equation. Solid line: $[\partial(\overline{u'w'})_A/\partial z]$, fine dashed line: $\partial(\overline{u'w'})_C/\partial z - \partial(\overline{u'w'})_A/\partial z$, dotted line: $\bar{u}(\partial\bar{u}/\partial x)$, dot-dashed line: $\bar{w}(\partial\bar{w}/\partial z)$, dashed line: $(1/\bar{\rho})(\partial\bar{p}/\partial x)$, where the overbar denotes averaging over 30 km.

suggests that in modeling convective (particularly slow-moving) lines, subgrid horizontal pressure gradients must be taken into account.

Although the FC parameterization allowed us to calculate mass and momentum fluxes, it had two deficiencies. The mass and momentum fluxes were underestimated, and vertical velocities in convective drafts were too large compared to those observed in GATE. We showed that underestimation of the mass flux and consequently, momentum flux was caused by an unrealistic mean mesoscale vertical velocity used in our calculations. This difficulty is avoided in an accurate numerical model. The overprediction of the vertical velocity in convective drafts causes the underestimation of the horizontal pressure gradient influence on momentum. The question of how the vertical velocity in convective drafts can be improved will be addressed in Part II.

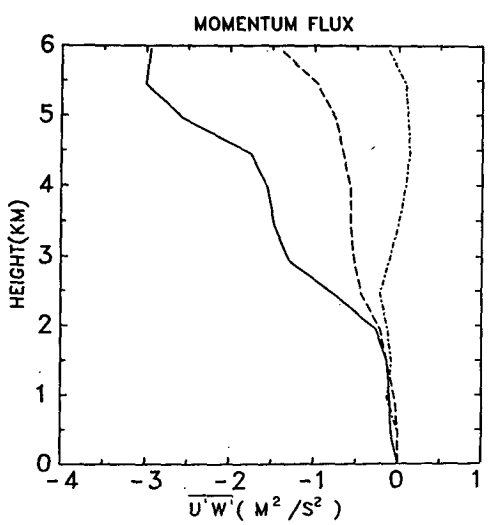

FIG. 18. Comparison of the $\overline{u'w'}$ momentum flux from the 14 September convective line (LeMone, 1983), averaged over first 30 km behind the leading edge (solid line) with the momentum flux calculated in the parameterization and corrected for observed mass flux with (dashed line) and without (dot-dashed line) horizontal pressure gradients.

There is one additional challenge in parameterization of momentum fluxes which needs to be solved. The subgrid-scale pressure gradients have to be calculated in the model, but parameterization using 1-D cloud model (as in FC) cannot serve this purpose. Therefore, the results of our study cannot be directly applied to the existing momentum flux parameterizations. Calculation of the subgrid horizontal pressure gradient must be consistently formulated in the cloud parameterization.

Acknowledgments. We would like to thank Dr. Margaret LeMone of the National Center for Atmospheric Research (NCAR) and Professor Richard Johnson for their reviews of this research and for helpful and inspiring discussions. We are grateful to Gail Watson carefully typing an earlier draft of this paper, and to our CSU colleagues for editorial assistance. This work was sponsored by the National Science Foundation under Grant ATM-8305759. Computing support was provided by the National Center for Atmospheric Research.

REFERENCES

Anthes, R. A., 1977: A cumulus parameterization scheme utilizing a one-dimensional cloud model. *Mon. Wea. Rev.*, **105,** 270–286.

Barnes, G. M., and K. Sieckman, 1985: The environment of fast and slow moving tropical convective cloud lines. *Mon. Wea. Rev.*, **112,** 1782–1794.

Beniston, M., 1984: A numerical study of atmospheric mesoscale cellular convection. *Dyn. Atmos. Oceans.*, **8,** 223–242.

Cotton, W. R., and R. A. Anthes, 1986: *Dynamic of clouds and precipitating mesosystems,* Chapter X, Academic Press, to be published.

Frank, J. M., and C. Cohen, 1985: Properties of tropical cloud ensembles estimated using a cloud model and observed cloud populations. *J. Atmos. Sci.*, **42,** 1911–1928.

Fritsch, J. M., and C. F. Chappell, 1980a: Numerical prediction of convectively driven mesoscale pressure systems. Part I: Convective parameterization. *J. Atmos. Sci.*, **37,** 1722–1733.

——, and ——, 1980b: Numerical prediction of convectively driven mesoscale pressure systems. Part II: Mesoscale model. *J. Atmos. Sci.*, **37,** 1734–1762.

Gamache, J. F., and R. A. Houze, Jr., 1983: Water budget of a mesoscale convective system in the tropics. *J. Atmos. Sci.*, **40,** 1835–1850.

LeMone, M. A., 1983: Momentum transport by a line of cumulonimbus. *J. Atmos. Sci.*, **40,** 1815–1834.

——, and E. J. Zipser, 1980: Cumulonimbus vertical velocity events in GATE. Part I: Diameter, intensity and mass flux. *J. Atmos. Sci.*, **37,** 2444–2457.

——, G. M. Barnes and E. J. Zipser, 1984: Momentum flux by lines of cumulonimbus over the tropical oceans. *J. Atmos. Sci.*, **41,** 1914–1932.

Raymond, D. J., 1984: A wave-CISK model of squall lines. *J. Atmos. Sci.*, **41,** 1946–1958.

Schneider, E. K., and R. S. Lindzen, 1976: A discussion of the parameterization of momentum exchange by cumulus convection. *J. Geophys. Res.*, **81,** 3158–3160.

Shapiro, L. J., and D. E. Stevens, 1980: Parameterization of convective effects on the momentum and vorticity budgets of synoptic-scale Atlantic tropical waves. *Mon. Wea. Rev.*, **108,** 1816–1826.

Stevens, D. E., 1979: Vorticity, momentum and divergence budgets of synoptic-scale wave disturbance in the tropical Eastern Atlantic. *Mon. Wea. Rev.*, **107,** 535–550.

Soong, S.-T., and W.-K. Tao, 1984: A numerical study of the vertical transport of momentum in a tropical rainband. *J. Atmos. Sci.*, **41,** 1049–1061.

Sui, C.-H., and M. Yanai, 1986: Cumulus ensemble effects on the large-scale vorticity and momentum fields of GATE. *J. Atmos. Sci.*, **43,** 1618–1642.

Yanai, M., S. Esbensen and J.-H. Chu, 1973: Determination of bulk properties of tropical cloud clusters from large-scale heat and moisture budgets. *J. Atmos. Sci.*, **30,** 611–627.

Zipser, E. J., and M. A. LeMone, 1980: Cumulonimbus vertical velocity events in GATE. Part II: Synthesis and model core structure. *J. Atmos. Sci.*, **37,** 2458–2469.